

Localization in a Nondegenerate Two-Dimensional Electron Gas

Philip W. Adams and Mikko A. Paalanen

AT&T Bell Laboratories, Murray Hill, New Jersey 07974

(Received 6 March 1987)

Magnetoresistance measurements of an electron gas formed on a solid-hydrogen substrate are reported as a function of surface disorder. High-mobility surfaces display an essentially classical positive B^2 field dependence. Lower-mobility surfaces, however, are characterized by the appearance of a negative magnetoresistance for fields less than ~ 0.2 T, in good agreement with present weak-localization theories. On extremely disordered surfaces we find large increases in resistivity but a finite residual electron diffusivity, $D \sim \hbar/m_{el}$.

PACS numbers: 73.20.Fz, 71.55.Jv

Two-dimensional electron gases (2DEG) formed on cryogenic surfaces have been studied intensely in recent years.^{1,2} These systems are not only attractive candidates for investigating the various phases of a 2D Coulomb gas,^{3,4} but they also provide a sensitive probe of the electron-substrate interaction and its role in electron transport. In the present Letter we report the first studies of localization in a nondegenerate 2DEG formed on a solid hydrogen substrate. Electron mobilities were varied over an order of magnitude, 6–0.2 m²/V·s, via impurity adsorption and a systematic study of the 2DEG magnetoresistance was made.

Electron transport in a disordered medium is generally divided into weak and strong localization. In the weak-localization regime, the scattering potential is treated perturbatively in $(kl)^{-1} \ll 1$ where k is the electron wave vector and l is the elastic mean free path. Weak-localization theory predicts that the coherence among multiple elastic-scattering paths of a single conduction electron will lead to an enhanced backscattering probability and a corresponding small negative correction to the conductance. The backscattering correction is limited by inelastic collisions and is of order $\Delta\sigma_{loc} \approx -(e^2/2\pi^2\hbar) \ln(\tau_i/\tau_0)$ in a 2D degenerate system,⁵ where τ_0 and τ_i are the elastic- and inelastic-scattering times, respectively. For the nondegenerate case the correction is proportional to T_F/T ,

$$\Delta\sigma_{loc} \approx (-\hbar n_0 e^2 / 2\pi k_B T m_{el}) \ln(\tau_i/\tau_0),$$

where n_0 is the electron density, and T_F is the Fermi temperature. Weak-localization theory is now on firm ground and has been verified in both degenerate electronic⁶ and electromagnetic systems.⁷ There are also conductivity corrections due to interaction effects which in a degenerate gas are of the same order as the single-electron effects. These, however, are proportional to $(T_F/T)^2$ in a highly nondegenerate system and are therefore completely negligible in the present study.⁸

Strong-localization theory addresses the case in which $kl \approx 1$. In this regime, electron transport is believed to be mediated either by thermally activated carriers in the

conduction band or by electron hopping. Several experiments⁹ support the existence of these mechanisms but no clear picture of how electrons go from being weakly localized to strongly localized has emerged.

There are several compelling advantages to the study of localization in a nondegenerate system. In practice, one would like to vary kl systematically from large values to $kl \approx 1$ while investigating the temperature or field dependence of the conductivity. Though this has been done in experiments on the inversion layer of metal-oxide-semiconductor field-effect transistors,⁶ these systems are generally limited to $kl \gtrsim 2$ and for technical reasons kl can only be varied by a factor of 5 or so for a given sample. The situation is much worse in light-scattering experiments where $kl \gtrsim 100$. In a nondegenerate system, however, the electron energies have a Boltzmann distribution, so that for a given energy-independent τ_0 , there are always electrons with $kl \lesssim 1$. Furthermore, since the density of states is constant in 2D, a substantial fraction of the distribution consists of low-energy electrons which can be easily localized. Finally, in contrast to a degenerate gas, $k_{thermal}$ and n_0 can be varied independently, allowing one to study essentially single-electron effects.

The response of the 2DEG was monitored in what is commonly known as a Corbino geometry which consisted of a 25-mm-diameter by 0.5-mm-thick sapphire plate placed upon a concentric-ring parallel-plate capacitor. Hydrogen crystals were grown on the sapphire at the triple point (~ 14 K) and electrons were deposited on the crystals via uv photoemission. The crystals were then cooled to liquid-helium temperatures over a period of several hours. All of the crystals were grown in ~ 1 Torr of helium to ensure good electron mobilities at 4.2 K. The helium was subsequently pumped out before the beginning of the measurements. The conductance of the 2DEG was monitored via its capacitive coupling to the detector¹⁰ and the electron density and average electron mobility were determined by application of a perpendicular magnetic field B . With neglect of localization effects, the classical (i.e., Drude) conductivity in a Cor-

bino geometry is $\sigma_{xx}(B) = \sigma_0/[1 + (\mu B)^2]$ where $\sigma_0 = n_0 e \mu$ is the zero-field conductivity and $\mu = e \tau_0 / m_{el}$ is the average electron mobility.

Shown in Fig. 1 are the magnetoresistance measurements for three different intrinsic surface disorders of a typical crystal with an initial electron density of $n_0 = 1.6 \times 10^{12} \text{ m}^{-2}$ and a corresponding Fermi temperature $T_F \approx 5 \text{ mK}$. The uppermost plot was made immediately after the crystal was cooled to 4.2 K and the lower two later, after the surface had degraded.¹¹ The dashed line in Fig. 1(a) represents the predicted classical magnetoresistance. The deviation from linearity is not quan-

tatively understood but does occur in the region of $\mu B = \omega_c \tau_0 \approx 1$ ($\omega_c \equiv$ cyclotron frequency), where one expects substantial modulation of the density of states due to the formation of Landau levels.⁹

Shown in Figs. 1(b) and 1(c) is the magnetoresistance of the crystal after one and two days, respectively. Note the substantial negative magnetoresistance at low fields and the positive B^2 dependence at higher fields. The negative magnetoresistance represents a suppression of the coherent backscattering by the magnetic field and the tail is essentially the classical $(\mu B)^2$ behavior. The field dependence of the weak-localization correction for a degenerate 2DEG is given by^{12,13}

$$\sigma_{xx} = \frac{-e^2}{\pi \hbar^2} \int_{E_c}^{\infty} \frac{dE}{1 + (\mu B)^2} \frac{\partial f(E)/\partial E}{\left\{ E \tau_0 - \frac{\hbar}{2\pi} \left[\Psi \left(\frac{\hbar m_{el}}{4eBE\tau_0^2} + \frac{1}{2} \right) - \Psi \left(\frac{\hbar m_{el}}{4eBE\tau_0\tau_i} + \frac{1}{2} \right) \right] \right\}}, \quad (1)$$

where Ψ is the digamma function, $f(E) = (\pi \hbar^2 n_0 / k_B \times T m_{el}) e^{-E/k_B T}$, and E_c is a lower-energy cutoff accounting for electrons with $kl \approx 1$ (or equivalently $E \tau_0 \approx \frac{1}{2} \hbar$). Note that the requirement that

$$E_c \geq (\hbar e / 2\pi m_{el} \mu) \ln(\tau_i / \tau_0) \quad (2)$$

is necessary to keep the integrand in Eq. (1) positive. The dashed and solid lines in Fig. 2 are predictions of Eq. (1) in which σ_0 , the first term in the integrand, has been factored out. The absolute conductivity was taken from the data and fits to the correction term were made in which μ and τ_i / τ_0 were varied with E_c given by Eq. (2) (dashed line). Somewhat better fits were achieved when E_c was treated as a fitting parameter (solid line).

The measurements in Fig. 1 were performed with a minimal amount of helium in the experiment cell. Electron scattering was, therefore, dominated by surface defects. We have also studied the case where electron scattering was dominated by ^4He atoms, by introducing

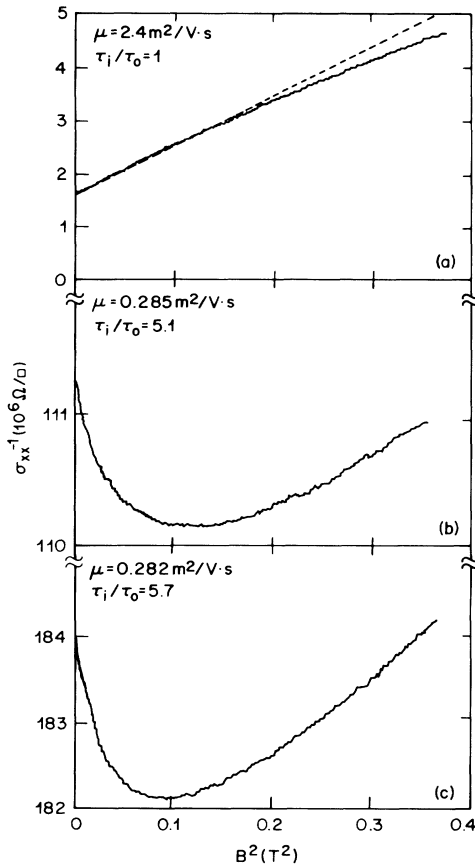


FIG. 1. Magnetoresistance of crystal No. 10 as a function of time, t , and increasing disorder at $T=4.2 \text{ K}$. (a) $t=2 \text{ h}$; (b) $t=24 \text{ h}$; (c) $t=48 \text{ h}$. The dashed line in (a) is the classical (Drude) prediction.

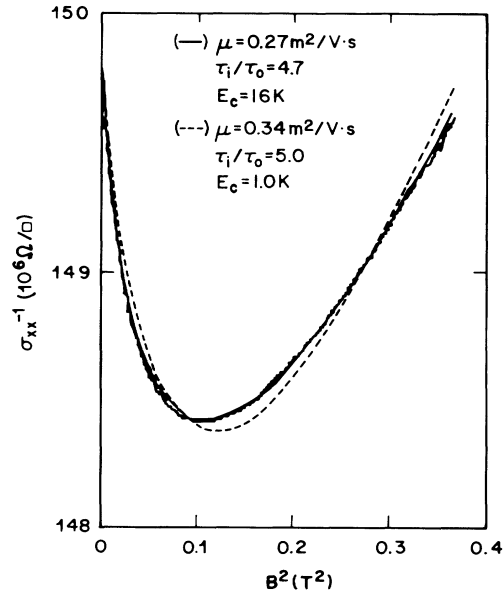


FIG. 2. Dashed line: Prediction of Eq. (1) in which μ and τ_i / τ_0 are varied for the best fit and E_c is given by Eq. (2). Solid line: Prediction of Eq. (1) in which μ , τ_i / τ_0 , and E_c are varied for the best fit.

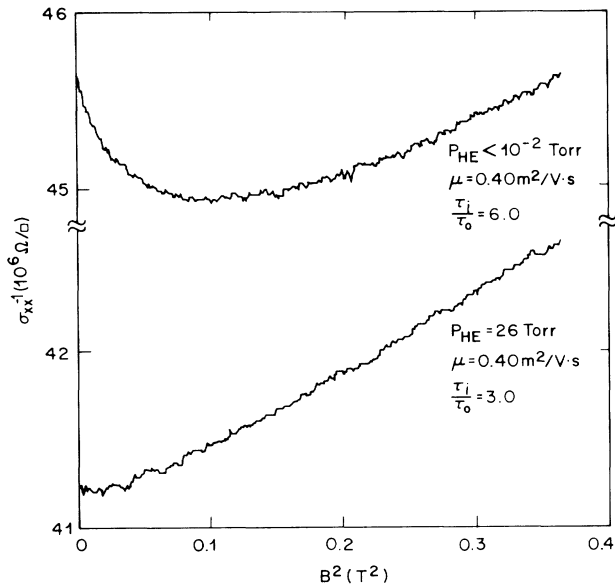


FIG. 3. Upper plot: The magnetoresistance with only a residual amount of ${}^4\text{He}$ in the cell. Lower plot: The magnetoresistance with $P_{\text{He}}=26$ Torr of helium in the cell.

helium gas onto a clean crystal surface. In Fig. 3 we have compared the magnetoresistances of two different crystals with and without ${}^4\text{He}$. In both cases the mobility, as determined from the high-field slope, are nearly identical, but the negative magnetoresistance in the case of ${}^4\text{He}$ scattering is considerably less. We interpret this as a reduction in the effective inelastic-scattering time due to both the recoil and the thermal motion of helium atoms.¹⁴ These two effects give rise to a dephasing time $\tau_w \lesssim \tau_0(m_{\text{He}}/m_{\text{el}})^{1/2}(kl)^{-1}$, which is generally small enough to destroy the coherence of the multiple scattering except for $kl \approx 1$.

We will now turn to the limit of extremely disordered surfaces and strong-localization effects in our data. We have plotted in Fig. 4 the conductivity of several crystals, normalized by the initial electron density, n_0 , as a function of the effective mobility as determined from fits to the high-field slope of the magnetoresistance. The solid line displays the expected classical relation $\mu = \sigma_0/en_0$ with constant carrier density and zero intercept. The data represented by the open circles were obtained by our lowering the mobility with helium gas which, in effect, introduces a large amount of inelastic scattering and tends to suppress localization effects. In contrast, the dark symbols represent data in which there was little helium in the system and substantially larger values of τ_i/τ_0 . Note that, in this case, σ_0/en_0 vanishes at a nonzero mobility and that this minimum mobility is higher at lower temperatures.

The decrease of σ_0 at a constant residual mobility, μ_{res} , can be interpreted as a decrease in the effective

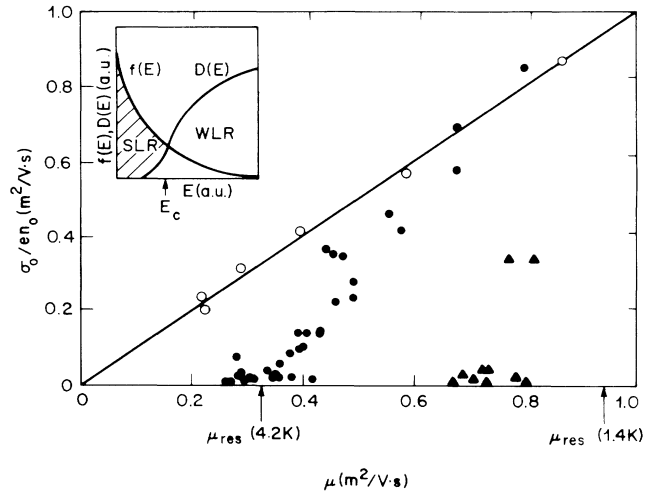


FIG. 4. The conductivity of several crystals normalized by the initial electron density as a function of mobility. Open circles: helium gas scattering, $T=4.2$ K; solid circles: without helium, $T=4.2$ K; solid triangles: without helium, $T=1.4$ K. The arrows are the prediction of Eq. (3). Inset: Diffusivity behavior, $D(E)$, folded in with the Boltzmann distribution, $f(E)$, near E_c . E_c demarcates the strongly localized (SLR) and weakly localized regimes (WLR).

mobile electron density, i.e., $\sigma_0 = en_{\text{eff}}\mu_{\text{res}}$. By the assumption that electrons below E_c do not contribute significantly to σ_0 , the integration over the Boltzmann distribution gives $n_{\text{eff}} \approx n_0 \exp(-E_c/k_B T)$. So as the crystal surface degrades E_c increases and more and more of the distribution freezes out. This is consistent with the observed monotonic decrease in n_{eff} with time ($n_{\text{eff}} < 10^{-4}n_0$ on extremely disordered surfaces).

In the following we present a qualitative argument for why σ_0 vanishes at a finite mobility and why Eq. (2) is not a good measure of E_c in the strongly disordered limit. When the substrate is only moderately disordered and the rms potential fluctuations, V_{rms} , are small with respect to $k_B T$ then the weak-localization cutoff is correct and E_c is, in fact, given by Eq. (2). However, when the surface becomes sufficiently rough so that $V_{\text{rms}} \gg k_B T$ then $E_c \approx V_{\text{rms}}$ and a large number of the electrons become strongly localized, substantially reducing the effective carrier density. In this limit, an electron with energy $E > E_c$ will, in general, be mobile but with an average kinetic energy measured relative to E_c , $E_k \approx \langle E - E_c \rangle \approx k_B T$. If one assumes that the surface disorder varies rapidly on the scale of such an electron's wavelength, λ , then it is not unreasonable to believe that the electron will scatter after traveling approximately one or a few reduced wavelengths and, on the average, not before. This is essentially the Ioffe-Regel condition. Taking $l \approx \lambda \approx (\hbar^2/m_{\text{el}}k_B T)^{1/2}$ and the thermal velocity $v \approx (k_B T/m_{\text{el}})^{1/2}$ we find that the electron diffusivity

$D \approx lv \approx \hbar/m_{\text{el}}$. By the Einstein relation, the residual mobility is

$$\mu_{\text{res}} \approx eD/k_{\text{B}}T \approx e\hbar/m_{\text{el}}k_{\text{B}}T \quad (3)$$

at the threshold of conduction. This is surprisingly close to the values shown in Fig. 4. The 1.4-K data are approximately 25% too low in mobility, but this is probably a consequence of residual helium contamination. The temperature dependence of μ_{res} has been verified in a striking experiment in which a relatively dirty crystal with a mobility of $\sim 0.3 \text{ m}^2/\text{V}\cdot\text{s}$ was cooled from 4.2 to 1.4 K. Though the conductance fell more than an order of magnitude, the mobility of the remaining conduction electrons increased to $\sim 0.7 \text{ m}^2/\text{V}\cdot\text{s}$!

In summary, we have investigated the effects of disorder on the transport properties of a Boltzmann distribution of electrons on hydrogen. We observe Drude behavior on clean crystals and both weak and strong localization on disordered surfaces. We find substantial evidence for a lower nonzero limit on the mobility on extremely disordered surfaces that is consistent with the requirement that $kl \sim 1$ at the threshold of conduction.

We are grateful to Dr. M. J. Stephen, Dr. S. Sachdev, and Dr. R. N. Bhatt for enlightening discussions and communications. We would also like to thank Dr. E. Abrahams and Dr. P. M. Platzman for helpful discussions.

¹K. Kajita and W. Sasaki, *Surf. Sci.* **113**, 419 (1982); A. M. Troyanovskii and M. S. Khaikin, *Zh. Eksp. Teor. Fiz.* **81**, 398 (1981) [*Sov. Phys. JETP* **54**, 214 (1981)].

²For a review of electrons on helium see F. I. B. Williams, *Surf. Sci.* **113**, 371 (1982).

³J. M. Kosterlitz and D. J. Thouless, *J. Phys. C* **6**, 1181 (1973).

⁴C. C. Grimes and G. Adams, *Phys. Rev. Lett.* **42**, 795 (1979).

⁵G. Bergmann, *Phys. Rev. B* **28**, 2914 (1983).

⁶D. J. Bishop, R. C. Dynes, and D. C. Tsui, *Phys. Rev. B* **26**, 773 (1982).

⁷M. P. Van Albada and A. Lagendijk, *Phys. Rev. Lett.* **55**, 2692 (1985); P. E. Wolf and G. Maret, *Phys. Rev. Lett.* **55**, 2696 (1985).

⁸S. Sachdev, unpublished.

⁹For a review see T. Ando, A. B. Fowler, and F. Stern, *Rev. Mod. Phys.* **54**, 437 (1982), Sect. V.

¹⁰See M. A. Paalanen and Y. Iye, *Phys. Rev. Lett.* **55**, 1761 (1985).

¹¹The degradation of the crystal surfaces occurred spontaneously over a period of a few days, which may have been the result of outgassing ($\text{H}_2, \text{N}_2, \text{O}_2$) in the large open volume of the experimental-cell pumping line or perhaps a roughening transition on the crystal surface.

¹²B. L. Altshuler, D. Khmel'nitzkii, A. I. Larkin, and P. A. Lee, *Phys. Rev. B* **22**, 5142 (1980).

¹³For simplicity, τ_0 and τ_i were assumed to be energy independent for $E > E_c$.

¹⁴M. J. Stephen, to be published.